Genome analysis of the unicellular eukaryote *Euplotes vannus* provides insights into mating type determination and tolerance to environmental stresses

Xiao Chen[1,2†], Yaohan Jiang[1†], Feng Gao[1*], Weibo Zheng[1], Timothy J. Krock[3], Naomi A. Stover[4], Chao Lu[2], Laura A. Katz[5], Weibo Song[1,6]

[1]Institute of Evolution & Marine Biodiversity, Ocean University of China, Qingdao 266003, China

[2]Department of Genetics and Development, Columbia University Medical Center, New York, NY 10032, USA

[3]Department of Computer Science and Information Systems, Bradley University, Peoria, IL 61625, USA

[4]Department of Biology, Bradley University, Peoria, IL 61625, USA

[5]Department of Biological Sciences, Smith College, Northampton, MA 01063, USA.

[6]Laboratory for Marine Biology and Biotechnology, Qingdao National Laboratory for Marine Science and Technology, Qingdao 266003, China

[†]Equal contributors

*Correspondence: E-mail: gaof@ouc.edu.cn

Abstract

Background:

The genus *Euplotes* is a clade of free-living and cosmopolitan ciliated protists. As a model organism in studies of cell and environmental biology, *Euplotes vannus* has more than ten mating types (sexes) and shows strong resistance to environmental stresses such as low temperature and high salinity. However, the molecular basis of its mating type determination mechanism and how the cell responds to stress are still largely unknown. Here we focus on these topics by genome analysis of different mating types of *Euplotes vannus*.

Results:

This work combines analysis of *de novo* assembled high-quality macronucleus (MAC; i.e. somatic) genome and partial micronucleus (MIC; i.e. germline) genome of *Euplotes vannus*. MAC genomic and transcriptomic data from several mating types of *E. vannus* were investigated and gene expression levels were profiled under different environmental stresses, including stresses from nutrient scarcity, extreme temperature, salinity and the presence of free ammonia. The results indicate that: 1) *E. vannus*, which possesses "gene-sized" nanochromosomes in its MAC, shares a similar pattern on frameshifting and stop codon usage as *Euplotes octocarinatus* and may be undergoing incipient sympatric speciation with *Euplotes crassus*; 2) *E. vannus* possesses two Type-I and four Type-II pheromones, including two novel alleles Ev-4 and Ev-beta, based on the genome investigation of six mating types; 3) the coding regions of pheromone genes in the MAC genome of *E. vannus* consist of multiple macronuclear destined sequences (MDS) regions in the MIC; 4) different mating types of *E. vannus* have mating type-specific chromatin and expression profiling of Type-II pheromone loci; 5) the HSP70 gene of *E. vannus* does not carry either unique amino acid substitutions of potential significance for cold adaptation nor mRNA destabilization ARE elements in its 3' regulatory region. Additionally, the genome resources generated in this study are available online at *Euplotes vannus* DB (http://evan.ciliate.org).

Conclusions:

Based on the results of the current study, the following conclusions are put forward: 1) the high similarity of the pheromones of *E. vannus* and *E. crassus* reveals the molecular basis of hybridization between these two "morphospecies" under laboratory conditions; 2) somatic pheromone loci of *E. vannus* are generated from programmed DNA rearrangements of multiple germline MDS segments, which are similar to the complex rearrangements of mating type determination in *Tetrahymena*; 3) however, unlike *Tetrahymena*, *E. vannus* does not possess mating type-specific genes. Instead, the mating types are distinguished by the different combinations of pheromone loci. This finding supports the allelic codominance or non-hierarchical dominance relationship among pheromone loci during *Euplotes* pheromone-mediated cell-cell signaling and cross-mating; 4) as a common species in global waters, the HSP70 gene of *E. vannus* has evolved to be insensitive to environmental temperature change.

Keywords:

Ciliated protist, DNA rearrangement, environmental stress, frameshifting, mating type determination.

Background

Single-celled, ciliated protists are abundant in diverse habitats across the globe, where they are among the most important components of food webs in aquatic ecosystems [1]. Ciliate diversity, physiology and abundance has been linked to studies of environmental change [2-4], pollution monitoring [5-8], biogeography [9-13], adaptive evolution [14-20] and epigenetics [21-23]. *Euplotes* is a genus of free-living marine ciliates that play important roles as both predators of microalgae and preys of multicellular eukaryotes like flatworms [24]. For decades, euplotids, including *Euplotes vannus*, have been widely used as model organisms in studies of predator/prey relationships [25-31], cell signaling [32, 33], toxicology of marine pollutants [34, 35] and experimental ecology [36-38]. For example, a previous molecular study revealed that *Euplotes* species have a large number of genes requiring +1 frameshifts (i.e. addition of base pairs post-transcriptional) for expression at the post-transcriptional level, which is much higher than viruses, prokaryotes and other eukaryotes [39].

Ciliates, including the models *Paramecium* and *Tetrahymena*, have been shown to present a wide variety of mating type numbers and modes of inheritance [40]. *Paramecium* has two mating types and its mating type determination (MTD) is controlled by scnRNA-dependent excision of the MTD gene promoter [41]. *Tetrahymena* has seven mating types, and different mating types specificities are encoded in the single pair of mating type genes in the MAC from all the six pairs in the MIC [42]. More than ten mating types have been identified in *Euplotes* [43-48], yet the molecular basis and MTD mechanism are unknown. Previous studies identified two subfamilies of mating-type specific pheromones in euplotids, a "shared" pheromone (designated Ec-alpha and named as Type-I pheromone in this work) and a "mating type-specific compositional" subfamily (designated Ec-1, Ec-2 and Ec-3, and named as Type-II pheromone) [49, 50]. They are considered as the key mediator during the cell-cell signaling that regulates cross-mating processes by controlling self/nonself recognition [51, 52]. Previous studies reported that the euplotid model implicates relationships of hierarchical (or serial) dominance among the pheromone alleles [53-55]. Yet the results from a recent work indicated that these pheromone genes were expressed without relationships of hierarchical dominance (i.e. heterozygous genotypes behaving like homozygous cells) in the *Euplotes* MAC genome [50].

Euplotids also feature a strong tolerance to environmental stresses. *Euplotes* spp. were reported to have a conserved molecular defense mechanism to heavy metal contamination for homeostasis by modulating mRNA expression [56]. In contrast, *E. crassus* and *E. focardii* had a barely detectable inducible HSP70 response to salinity and temperature stresses [14, 57]. These findings add weight to the argument that the lack of the classical heat shock response might be an adaptation strategy of euplotids to extreme environmental stresses. Additional studies reported *E. vannus*, as a microzooplanktonic grazer, had considerably strong tolerance to ammonia, which may enable it to survive in intensive aquaculture ecosystems with high levels of ammonium, potentially causing great damage in microalgal industry [36, 37]. Thus, it is important to elucidate the molecular mechanism of *Euplotes* cell response to external stresses under the background of global warming.

In this work, we analyze genomic and transcriptomic data of different mating types of *E. vannus* to study its genomic features, which lead us to reveal the molecular basis of mating type determination in euplotids. Furthermore, the gene expression profiling of *E. vannus* cells under different environmental stresses allows us to evaluate how this species tolerates the varying harsh conditions that it encounters.

Results

General description of genome sequencing and assembly of *Euplotes vannus*

In the current work, we acquired the MAC genomic data of four different mating types (EVJ, EVK, EVL and EVM), which were experimentally confirmed (Table S1). The MAC genome assemblies of these mating type had an average size of 164.2 Mb with a mean coverage of 61X (Table 1 and supplementary information, Figure S1 and Table S2).

After the contigs identified as noise (coverage < 5X) or contamination of bacteria and mitochondria were removed, the final genome assembly of *E. vannus* was generated by merging the genome assemblies of these four mating types (assembled genome size is 85.1 Mb and N50 = 2,685 bp, Table 1). We compared these data with those of two other euplotids, *E. crassus* and *E. octocarinatus*. Although *E. vannus* and *E. crassus* shared a

similar %GC (36.95% and 38.65%, respectively), the genome size, number of 2-telomere contigs and N50 value of *E. vannus* were more comparable with those of *E. octocarinatus* (Table 1).

The contig N50 values of these three *Euplotes* species were all smaller than 3 kb, because chromosomes of *Euplotes* species are "nanochromosomes", similar to that of *Oxytricha trifallax* [39]. The 2-telomere contig percentage of the merged genome of *E. vannus* is 66.7%, consistent with *E. octocarinatus* in which 70.3% contigs contained telomeres on both ends. Among the four mating types with genomic sequencing data, the genome assembly of EVJ was of highest quality with a 2-telomere contig percentage of 81.6% and N50 of 2,954 bp (Supplementary information, Table S2).

To evaluate the completeness of the genome assembly of *E. vannus*, gene content from single-copy orthologs of protists was identified by BUSCO, and the result indicated that the current assembly had a comparable percentage of complete ortholog sequences with other species (Figure 1 and supplementary information, Figure S2). Furthermore, the majority of genomic DNA sequencing reads of four mating types (EVJ, EVK, EVL and EVM) and RNA-seq reads of six mating types (EVJ, EVK, EVL, EVM, EVP and EVX) in both starvation and vegetative stages can successfully be mapped back to the merged reference genome assembly with a mean mapping ratio of 80.1% (Supplementary information, Table S3). Furthermore, 109 tRNAs which consist of 48 codon types for 21 amino acids, were detected in the final genome assembly (Supplementary information, Table S4). These results indicated that our genome assembly of *E. vannus* was largely complete. The information of repeat regions and functional annotation of genes are summarized in supplementary information, Figure S3, Table S5 and Table S6.

The size distribution of complete chromosomes of *E. vannus* (i.e. those bearing telomeric repeats "C4A4" and "T4G4" on both ends) is quite close to that of another two euplotids, *E. octocarinatus* and *E. crassus*, with the peak values around 1.5 kb (Figure 1B). A similar result was found in the size distribution of telomeres, in which most telomeres of all three euplotids had a length of 28 bp, with an increment of 8 bp (Figure 1C). Most identified *E. vannus* introns were around 25 bp in length, with a canonical sequence motif 5'-GTR(N)nYAG-3' at either end (Figure 1DE and supplementary information, Figure S4).

Evolution and synteny/comparative genomic analyses among euplotids

"Joint" nanochromosomes

Most chromosomes (37501/38245, 98.1%) in *E. vannus* are nanochromosomes, or so-called gene-sized chromosomes, bearing a single gene on each. A similar result was observed in *E. octocarinatus* (40396/41980, 96.2%). There was a small proportion of chromosomes that contains more than one gene (Figure 2A). These "joint" nanochromosomes were then divided into two groups by the consistency and inconsistency of the transcription directions of the genes on them (cis and trans, respectively). The trans-joint nanochromosomes had close numbers, considering the total chromosome numbers were similar in these two euplotids (Table 1). However, *E. octocarinatus* possessed 2-fold more cis-joint nanochromosomes than *E. vannus*.

Homologous genes

E. vannus and *E. crassus* shared 25026 closely related contigs (E-value cutoff = 1e-5), which was equivalent to 65.4% and 44.2% of total contigs for each species, respectively (Figure 2B). However, only 469 contigs were shared between these two species and *E. octocarinatus*. Furthermore, *E. vannus* and *E. crassus* shared not only more homologous contigs, but also more sequence identity (Figure 2C). For example, the sequence identity between *E. vannus* and *E. crassus* of the corresponding region on the chromosome that contains the coding gene of dynein heavy chain protein was 99.6%, while the sequence identity between *E. vannus* and *E. octocarinatus* was 71.2%.

Frameshifting

Frameshifting events in *E. vannus* and *E. octocarinatus* were detected by identifying the adjacent region between two BLASTX hits that are in different frames, targeting to a same protein sequence (illustrated by supplementary information, Figure S5). The E-value cutoff (1e-5) ensured the accuracy of the prediction process and a small inner distance cutoff (10 nt) was applied to get rid of the interference from introns, because all introns of euplotids were larger than 20 nt as described above (Figure 2D). The result indicated that the high frequency of +1 programmed ribosomal frameshifting (PRF) was a conserved feature in

192 euplotids. However, intriguingly, more +2 and -1 PRF events were found in *E. vannus*
193 (16.6%) than in *E. octocarinatus* (4.4%). With more cases of +2 and -1 PRF events being
194 spotted, a novel motif rather than the canonical motif 5'-AAA-TAR-3' (R = A or G) was
195 revealed as 5'-WWW-TAR-3' (W = A or T) (Figure 2E).

196

197 *Stop codon usage*

198 Based on the genomic and transcriptomic sequencing data, the stop codon usage was
199 analyzed in *E. vannus* and *E. octocarinatus* and compared between the regular transcripts
200 and the slippery sites of PRF transcripts (Figure 2F). In these two euplotids, UAA was
201 preferentially used in the regular termination signal (73.7% and 76.0%, respectively) and in
202 the slippery signal (91.3% and 91.0%, respectively). Moreover, the frequency of UAA
203 codon usage in slippery signal is significantly higher than that in the regular termination
204 signal (p = 0.005024 < 0.01, Analysis of variance), which suggested that UAA may be
205 favorable for frameshifting in both *E. vannus* and *E. octocarinatus*.

206

207 Profiling and development of *Euplotes* pheromone genes

208 Pheromone alleles were successfully identified in MAC genomes of four *E. vannus* mating
209 types (Supplementary information, Table S7). Other than the pheromones Ev-1, Ev-2, Ev-3
210 and Ev-alpha that were orthologous to Ec-1, Ec-2, Ec-3 and Ec-alpha in *E. crassus*,
211 respectively, a novel Type-II pheromone Ev-4 and a novel Type-I pheromone Ev-beta were
212 found in *E. vannus* (Figure 3A and supplementary information, Figure S6, Figure S7 and
213 Figure S8). Although Ev-4 used "TAG" as stop codon rather than using "TAA" in other
214 three Type-II pheromones (Supplementary information, Figure S6), together with Ev-beta,
215 they showed a significant sequence similarity with the other three known pheromones,
216 especially in the pre- and pro-regions of the cytoplasmic precursor (marked by red arrows
217 in Figure 3A) and retained highly conserved cysteine residues in the secreted region
218 (marked by red dots), which was an important feature of pheromone allele sequences.

219 The phylogenetic analysis of *Euplotes* pheromones, including the homologs in each
220 mating type of *E. vannus* and the corresponding consensus sequences, was performed
221 (Figure 3A). Although these MAC loci were generated by alternative processing of MIC

222 regions in each species, the result indicated that the pheromones of *E. vannus* clustered
223 together with those of *E. crassus*, distinct from those of other Euplotids, *E. octocarinatus*, *E.*
224 *nobilii* and *E. raikovi*.

225 Chromatin profiling of pheromone genes indicated that the combination of Type-II
226 pheromone genes, Ev-1, Ev-2, Ev-3 and Ev-4, exhibited a mating type-specific feature on
227 genic level (Figure 3B and supplementary information, Figure S9). Different mating types
228 retained 1-3 Type-II pheromone genes in the MAC genome and no duplicate events
229 existed. Gene expression profiling of pheromone genes consistently showed that both two
230 Type-I pheromones Ev-alpha and Ev-beta were highly expressed in all six mating types in
231 *E. vannus* and confirmed the mating type-specific chromatin profiling of Type-II pheromone
232 genes in different mating types at the transcriptional level. As another independent
233 verification, PCR amplification of pheromone loci was carried out to verify the presence of
234 the pheromone-related contigs in the MAC genome of each mating type (Figure 3C). The
235 results of PCR amplification of pheromone loci indicated that Type-II pheromone gene Ev-
236 1 was absent from the mating types EVL, EVM and EVP, Ev-2 was absent from EVK, EVM,
237 EVP and EVX, Ev-3 was absent from EVJ and Ev-4 was absent from EVK and EVP, which
238 were mostly consistent with the results from chromatin and gene expression profiling
239 (Figure 3B). In brief, each of the six mating types we identified contained a unique
240 combination of four Type-II pheromone genes.

241 To further study the development process of the pheromone genes during the
242 programmed DNA rearrangement from germline MIC to somatic MAC in *E. vannus*, MIC
243 genomic DNA was acquired by single-cell sequencing and its draft genome was
244 assembled (Table 2). Then the germline genome (MIC) origins of Ev-1 (MAC Contig16568),
245 Ev-2 (Contig28896), Ev-3 (Contig29423) and Ev-4 (Contig34058) were mapped to MIC
246 contigs (Figure 3C and supplementary information, Table S8, E-value cutoff = 1e-5). The
247 coding region of pheromone genes Ev-1, Ev-2 and Ev-3 consisted of three MDS regions
248 from the MIC genome while Ev-4 consisted of at least two MDS regions. However, the
249 germline source of a part of the pro-region and the secreted region of Ev-4 was not found.

250

251 Molecular basis of strong tolerance to extreme environmental stresses

Stress from nutrient scarcity: starvation-induced and mating type-specific transcripts

Starvation stress (i.e. nutrient scarcity) had limited impact on the expression pattern of different mating types by global transcription profile (Figure 4A and supplementary information, Figure S10). However, differential gene expression analysis revealed some mating type-specific transcripts under nutrient scarcity (Figure 4B). Transcripts induced by starvation tended to be associated with mating type-specific genes (42.8%; see supplementary information, Figure S11). Gene functional annotation reveals that these starvation-induced and mating type-specific transcripts are related to protein transport and phosphorylation process in cells (Figure 4C and supplementary information, Figure S12). The expression of these genes may facilitate the cell response to pheromone-mediated cell-cell signaling and cross-mating behavior under the stress from nutrient scarcity.

Stresses from extreme temperature, salinity or the presence of free ammonia

PCA analysis based on the differential gene expression of *E. vannus* EVJ cells under different extreme environmental stresses was performed (Supplementary information, Figure S13A). The result revealed changes in the gene expression profile of cells under high temperature (35 ^{o}C), low temperature (4 ^{o}C), high or low salinity (60 and 10 psu, respectively). Also, the presence of free ammonia had substantial impact on transcription patterns (Supplementary information, Figure S13). Surprisingly, cells under high salinity and low salinity shared a similar gene expression profile (Supplementary information, Figure S13A).

To further dissect the relationships between co-expression of genes associated with the regulation of cellular processes and pathways under extreme environmental changes, a weighted gene co-expression eigengene network was constructed (Figure 5A). The network clustered different eigengenes into six modules based on their co-expression profile (Supplementary information, Figure S13B). A strongly co-expressed eigengene module was up-regulated in cells under both high and low salinity stresses (colored in steel blue in Figure 5A and supplementary information, Figure S13B). This module was involved with an extensive activation of many pathways, mainly related to tRNA aminoacylation, tRNA and rRNA processing, nucleosome assembly and pseudouridine synthesis (p.adjust

< 0.05). In addition, two small eigengene modules were up-regulated in cells under high salinity stress (purple) and low salinity stress (dark green), respectively, and low salinity stress activated an extra pathway related to the glutamine metabolic process.

Intriguingly, low temperature stress induced a large module cluster of eigengenes related to small GTPase mediated signal transduction, while very few eigengenes co-expressed under the high temperature (blue and purple, respectively, in Figure 5 and supplementary information, Figure S13B). The homolog of the highly conserved heat-shock protein 70 (Hsp70), which many organisms upregulate under environmental stress, was identified in *E. vannus* and compared with its counterparts in *E. nobilii* and *E. focardii* (Figure S14). The result revealed that only the *E. focardii* Hsp70 sequence had numerous amino acid substitutions within its two major functional domains, i.e. the ATP-binding and substrate-binding domains (Figure 6A). However, the transcription of the HSP70 gene in *E. vannus* did not respond to temperature stresses while being responsive to other stresses like salinity and chemical stresses (Figure 6B).

To gain a better understanding of the molecular basis of the lack of change in response of the HSP70 gene to temperature stress in *E. vannus*, we analyzed the structure of non-coding regions flanking the gene in *E. vannus* and compared the structure of this gene between *E. vannus* and *E. focardii* (Figure 6CD). The result indicated that no substantial difference was detected in the 5' promoter region between the HSP70 genes of these two species, both bearing canonical regulatory *cis*-acting elements that bind transcriptional trans-activating factors, including heat-shock elements (HSE) and stress-response elements (StRE) (Figure 6C). Furthermore, neither *E. vannus* nor *E. focardii* retained mRNA destabilization ARE elements in their 3' promoter region (Figure 6D).

The gene expression of cells under the presence of free ammonia were very similar to those under high temperature stress, and there was a small cluster of eigengenes that responded related to the lipid metabolic process (Figure 5 and supplementary information, Figure S13B). However, chemical stress activated the expression of HSP70 gene in *E. vannus* significantly (Figure 6B).

Discussion

Genomes of ciliates are divergent to each other and largely unexplored

Besides euplotids, we also evaluated the assembly completeness of genomes or transcriptomes of other ciliates and found a large divergence among them (Figure 1A and supplementary information, Figure S2). It reflects two facts: 1) ciliates have great genetic distances, even those closely related on phylogeny; 2) ciliate genomic data sequenced so far has not been collected by assembly completeness evaluation tools like BUSCO (the only ciliate covered is *Tetrahymena thermophila*). Nevertheless, among these ciliates, the completeness of transcriptome assembly of three species, *Anophryoides haemophila*, *Uronema* sp. and *Condylostoma magnum*, were not evaluated. One of the most likely reasons is that they possess small genome volume and thus share few genes with other ciliates [58]. For instance, *Anophryoides* and *Uronema* are well-known parasitic species that cause disease in fish and lobsters in aquaculture facilities and have very small genome sizes [59-63]. Another reason is that stop codon rearrangement occurs in some ciliates, such as *Condylostoma magnum*, all standard stop codons are reassigned to amino acids in a context-dependent manner [64, 65]. These unusual features could dramatically increase the difficulty to precisely evaluate the assembly completeness of ciliate genomes/transcriptomes. Overall, the genomic investigation in ciliates is still waiting to be explored and the evaluation of ciliates genome assemblies calls for further improvement.

Molecular basis of the mating type determination in *E. vannus*

Genomic data and pheromone gene assay supports the hypothesis that E. vannus and E. crassus may be undergoing incipient sympatric speciation

An early study reported that *E. vannus* could interbreed with *E. crassus* under laboratory conditions [66]. Other studies reported that *E. vannus* and *E. crassus* might be undergoing sympatric speciation [67, 68]. The result in the current work increased the weight of this argument in three aspects: 1) *E. vannus* and *E. crassus* are closely clustered with each other among euplotid species (Figure 1A); 2) these two species shared both a large number of homologous sequences and at high levels of sequence identity, in contrast to

342 comparisons with *E. octocarinatus* (Figure 2BC); 3) the homologs of pheromones of *E.*
343 *vannus* and *E. crassus* are closely related and distinct from those from other *Euplotes*
344 species (Figure 3AB). Orthologs of each pheromone allele from different mating types of *E.*
345 *vannus* shares identical sequences on both gene and protein levels in most cases except
346 pheromone gene Ev-2 (Figure 3A and supplementary information, Figure S6, Figure S7
347 and Figure S8). Our findings might describe a pattern that mating type loci evolve rapidly
348 after a recent speciation between *E. crassus* and *E. vannus*.

349

350 *The combination of Type-II pheromone loci is mating type-specific in E. vannus MAC*

351 Type-I pheromone Ec-alpha has large sequence differences with the Type-II pheromones
352 and has been considered as an "adaptor" that interacts with the other pheromones, as it
353 has a strong propensity to oligomerize and retains a hydrophilic domain for putative
354 interaction [50, 52]. This argument is supported by the results of expression profiling for
355 pheromone genes in the current work (Figure 3B).

356 Studies on the pheromones from other euplotids, including *E. raikovi* [69-75], *E.*
357 *nobilii* [51, 76-78] and *E. octocarinatus* [79-82], revealed that highly enriched and
358 conserved cysteine residues in secreted region is the most outstanding sequence motif of
359 *Euplotes* pheromones [52]. The novel pheromone Ev-4 identified in this study from *E.*
360 *vannus* retains 10 cysteines, as same as other Type-II pheromones in *E. vannus* and *E.*
361 *crassus*, and thus matches this characteristic perfectly (Figure 3A).

362 As the Ec-1 and the other two Type-II pheromones, Ec-2 and Ec-3, were identified
363 in different mating types of *E. crassus* by pheromone purification and molecular mass
364 determination after chromatographic separation, confirmed by PCR amplification and
365 sequencing, Type-II pheromones have been considered as mating type-specific [49, 50].
366 However, our study demonstrated that six *E. vannus* mating types retain different
367 combinations of Type-II pheromone loci in their MAC genomes (Figure 3C), and thus they
368 exhibited highly different pheromone gene expression profiling instead of possessing
369 exclusive, mating type-specific genes (Figure 3B). Furthermore, mating types EVL and
370 EVP have the same set of pheromone genes but with different abundance (Figure 3C).
371 Therefore, it suggests that the mating type-specific combination of the Type-II pheromone

loci might not be an all-or-none phenomenon, but a manner related to the composition or copy number of Type-II pheromone genes. Although further studies are expected, the observations of mating type-specific combination in the current study support the allelic codominance or non-hierarchical dominance relationship among signaling pheromone genes in euplotids [50, 52].

A new model for mating type determination in ciliates

Taken together, the current work revealed that euplotids have a novel MTD manner by which mating types are determined through mating type-specific combination of four Type-II pheromone genes (Figure 7C). Unlike *Paramecium tetraurelia*, there is no excision event on promoter regions of *E. vannus* pheromone genes (Figure 3C, Figure 7A and supplementary information, Figure S6). On the other hand, the MAC of *E. vannus* does not possess exclusive mating type-specific MTD loci as *Tetrahymena thermophila* (Figure 3 and Figure 7B). This mating type-specific feature of Type-II pheromones comes from the programmed DNA rearrangement between germline and somatic genomes. Intriguingly, none of the *E. vannus* mating types we have identified possesses all four Type-II pheromone genes in MAC (Figure 3B and supplementary information, Figure S9). Thus, the results of current study described a third MTD type in ciliate (Figure 7C).

Molecular basis of the HSP70's lack of response to temperature stress

A previous study indicated that response of the HSP70 gene expression to temperature change, no matter gradually or abruptly, was divergent between *E. nobilii* and *E. focardii* [14]. When transferred from 4 to 20 ºC, a strong transcriptional activity of HSP70 genes was induced in *E. nobilii* cells, while no measurable change was found in cells of *E. focardii*. In contrast, HSP70 expression increased with oxidative and chemical stresses such as tributyltin and sodium arsenite [15]. Furthermore, together with the results from the previous studies [67, 83], the current work strongly suggest HSP70 gene of *E. vannus*, which is largely divergent from that of with *E. focardii*, does not carry unique amino acid substitutions of potential significance for cold adaptation (Figure 6A).

401 The cosmopolitan species *E. vannus* has a similar pattern of HSP70 gene activation
402 to the Antarctic psychrophilic euplotid *E. focardii*, in contrast to the euplotid *E. nobilii* in
403 which the HSP70 gene expression changed with both thermal and chemical stresses
404 (Figure 6B). A previous study reported no substantial difference in the organization of the
405 HSP70 5' promoter region between *E. focardii* and *E. nobilii*, but an adenine-rich element
406 which would exclude a rapid mRNA degradation was detected in the HSP70 3' regulatory
407 region of *E. nobilii* [16]. In both two euplotids, the 5' promoter region harbors the *cis*-acting
408 elements like heat-shock elements (HSE) and stress-response elements (StRE), which are
409 known to be targets of trans-acting transcriptional activators characterized in a variety of
410 organisms in association with their stress-inducible genes [84-86]. It's also argued that the
411 HSE-modulated HSP70 gene transcription is more specific for a response to temperature
412 stress while the StRE-modulated HSP70 gene transcription is more specific for a response
413 to a broader range of non-temperature stresses [16]. Combining these data with
414 observations in the current work, we argue that structural divergence of transcriptional
415 *trans*-activating factors underlies that lack of change of HSP70 gene expression in
416 response to temperature stress in *E. vannus* and *E. focardii*

417

418

419 **Conclusions**

420 In the current work, we present a high-quality macronuclear and a partial micronuclear
421 genome assemblies of a unicellular eukaryote, *Euplotes vannus*, which possesses "gene-
422 sized" MAC nanochromosomes. Comparative genome analysis reveals that *E. vannus*
423 shares similar pattern on frameshifting and stop codon usage with *E. octocarinatus* and is
424 undergoing incipient sympatric speciation with *E. crassus*. The further investigation on
425 *Euplotes* pheromones indicates that *E. vannus* has a set of orthologous pheromones with
426 the reported ones in *E. crassus* as well as a novel type of pheromone named as Ev-4
427 which also shares close homology with *E. crassus*, and thus explains the hybridization
428 between these two species on the molecular level. Besides, the homologous search
429 between MAC and MIC genomes reveals that pheromone genes in *E. vannus* develop by
430 programmed DNA rearrangement. Furthermore, chromatin and expression profiling of
431 pheromone genes indicated that the combination of these genes is mating type-specific on

genic level and thus provides new evidence for common pheromone-mediated cell-cell signaling and cross-mating. According to the analyses of transcriptomes under different environmental stresses, although the HSP70 gene of *E. vannus* does not carry unique amino acid substitutions of potential significance for cold adaptation, it has evolved to be insensitive to temperature change by losing mRNA destabilization ARE elements in the 3' regulatory region of HSP70.

Methods

Cell culture

Six mating types of *Euplotes vannus* (EVJ, EVK, EVL, EVM, EVP and EVX) were collected from seawater along the coast of Yellow Sea at Qingdao (36°06′ N, 120°32′ E), China. Cells of each mating type were cultured separately in filtered marine water at 20°C for 10 days, with a monoclonal population of *Escherichia coli* as the food source, until reaching 10^6 cells.

Experimental treatment simulating environmental stresses

To simulate the stress from nutrient scarcity, 10^6 cells of each mating type (EVJ, EVK, EVL, EVM, EVP and EVX) of *E. vannus* were starved for 24 hours before harvest. For stresses from low and high temperature, 10^6 cells of *E. vannus* mating type EVJ were cultured under the temperature of 4 ^{o}C and 35 ^{o}C, respectively, for 6 hours before harvest. For stress from low and high salinity, 10^6 cells of mating type EVJ were cultured under the salinity of 10 psu and 60 psu, respectively, for 6 hours before harvest. For stress from the presence of free ammonia, 10^6 cells of mating type EVJ were cultured in filtered marine water with 100 mg/L NH_4Cl (pH 8.3, 20 ^{o}C and 35 psu), as described in the previous study [36]. Cells in two negative control groups were culture under pH 7.8 and pH 8.2, respectively, in filtered marine water under 20 ^{o}C and 35 psu. Each group had two biological replicates.

High-throughput sequencing and data processing

For regular genomic and transcriptomic sequencing to acquire macronucleus (MAC) genome information, cells were harvested by centrifugation at 300 g for 3 min. The genomic DNA was extracted using the DNeasy kit (QIAGEN, #69504, Germany). The total RNA was extracted using the RNeasy kit (QIAGEN, #74104, Germany) and digested with DNase. The rRNA fraction was depleted using GeneRead rRNA Depletion Kit (QIAGEN, #180211, Germany).

For single-cell whole-genome amplification to acquire micronucleus (MIC) genome information, a single vegetative cell of the mating type EVJ of *E. vannus* was picked and washed in PBS buffer (without Mg^{2+} or Ca^{2+}) and its MIC genomic DNA was enriched and amplified by using REPLI-g Single Cell Kit (QIAGEN, #150343, Germany), which was based on the whole-genome amplification (WGA) technology and tended to amplify longer DNA fragments.

Illumina libraries were prepared from amplified single-cell MIC genomic DNA of *E. vannus* according to manufacturer's instructions and paired-end sequencing (150 bp read length) was performed using an Illumina HiSeq4000 sequencer. The sequencing adapter was trimmed and low-quality reads (reads containing more than 10% Ns or 50% bases with Q value <= 5) were filtered out.

Genome assembly and annotation

Genomes of four mating types (EVJ, EVK, EVL and EVM) were assembled using SPAdes v3.7.1 (-k 21,33,55,77), respectively [87, 88]. Mitochondrial genomic peptides of ciliates and genome sequences of bacteria were downloaded from GenBank as BLAST databases to remove contamination caused by mitochondria or bacteria (BLAST E-value cutoff = 1e-5). CD-HIT v4.6.1 (CD-HIT-EST, -c 0.98 -n 10 -r 1) was employed to eliminate the redundancy of contigs (with sequence identity threshold = 98%) [89]. Poorly supported contigs (coverage < 5 and length < 300 bp) were discarded by a custom Perl script.

A final genome assembly of *E. vannus* was merged from the genome assemblies of four mating types (EVJ, EVK, EVL and EVM) by CAP3 v12/21/07 [90]. Completeness of genome assembly was evaluated based on expectations of gene content by BUSCO v3

(dataset "Alveolata") and the percentage of both genomic and transcriptomic reads mapping to the final assembly by HISAT2 v2.0.4 [91, 92]. Reads mapping results were visualized on GBrowse v2.0 [93]. Genome assemblies of *E. crassus* (accession numbers: GCA_001880385.1) and *E. octocarinatus* (accession numbers: PRJNA294366) and their annotation information were acquired from NCBI database and the previous studies [39, 94, 95].

Telomeres were detected by using a custom Perl script which recognized the telomere repeat 8-mer 5'-(C4A4)n-3' at the ends of contigs, as described in a previous study [96]. The repeats in the merged genome assembly were annotated by combining *de novo* prediction and homology searches using RepeatMasker (-engine wublast -species '*Euplotes vannus*' -s -no_is) [97]. *De novo* genome-wide gene predictions were performed using AUGUSTUS v3.2.2 (--species = euplotes, modified from the model "tetrahymena", rearranging TAA/TAG as stop codon, TGA as Cys) [98]. ncRNA genes were detected by tRNAscan-SE v1.3.1 and Rfam v11.0 [99, 100].

Gene modeling and functional annotation

After mapping RNA-seq data of each mating type of *E. vannus* back to the merged reference genome assembly, the transcriptome of six mating types as well as a merged transcriptome were acquired by using StringTie v1.3.3b [101]. Annotation of predicted protein products were matched to domains in Pfam-A database by InterProScan v5.23 and ciliate gene database from NCBI GenBank by BLAST+ v2.3.0 (E-value cutoff = 1e-5) [102, 103].

Comparative genomic analysis

BLAST+ v2.3.0 was employed to search ciliate gene database from NCBI GenBank to identify corresponding homologous sequences in euplotids (E-value cutoff = 1e-1 and match length cutoff = 100 nt) [103]. "Joint" chromosomes were detected by using a custom Perl script which recognized the chromosomes containing multiple genes (cutoff of distance between two genes = 100 nt). Frameshifting events were detected by using a custom Perl script which recognized the frame change between two BLASTX hits (E-value

cutoff = 1e-5 and inner distance <= 10 nt), modified from the protocol in a previous study [39], with the addition of a strict criterion (the distance between two adjacent hits with different frames <= 10 bp) to make sure no intron was involved. 30 bp sequences from the upstream and downstream of each type of frameshifting site (+1, +2 or -1) were extracted to identify the motif. Local motifs of nearby frameshifting sites were illustrated by WebLogo 3 [104]. The frequency of stop codon usage was estimated by a custom Perl script which recognized the stop codon TAA or TAG in transcripts of euplotids.

Differential gene expression analysis

Transcript abundances were estimated and differential gene expression was analyzed by using featureCounts [105] and R packages "Ballgown" and "DESeq2" (p.adjust < 0.01) [106, 107]. Starvation induced genes were defined as the average value of RPKM of gene expression from starved samples > 1 and the average value of RPKM of gene expression from vegetative samples < 0.1. Mating type-specific transcripts were defined as the average value of RPKM of gene expression from starved samples > 5 and the average value of RPKM of gene expression from vegetative samples < 0.1. Weighted gene co-expression eigengene network analysis was performed by WGCNA [108]. Gene Ontology (GO) term enrichment analysis was performed by using BiNGO v3.0.3 (p.adjust < 0.05), which was integrated in Cytoscape v3.4.0, and the plot was generated by the R package, ggplot2 [109-111].

Homolog detection of pheromone genes and environmental stress-related genes

Homologous pheromone gene sequences in *E. vannus* were acquired by using BLAST+ v2.3.0 (E-value cutoff = 1e-5), according to the pheromone sequences of *E. crassus* [49, 50]. Genomic DNA samples were harvested from vegetative cells of six mating types of *E. vannus*. Type-II pheromone loci in MAC were amplified using Q5 High-Fidelity 2X Master Mix (NEB, #M0492S, US) with 10 cells of each mating type and genotyping primers (PCR annealing temperature was 64.5 ^{o}C, sequences of genotyping primers see supplementary information, Table S9).

Homologous HSP70 gene sequences in *E. vannus* was acquired by using BLAST+ v2.3.0 (E-value cutoff = 1e-5), according to the Hsp70 protein sequences of *E. focardii* and *E. nobilii* from the previous studies (GenBank accession number: AAP51165 and ABI23727, respectively) [14, 16]. The complete sequences of the *E. focardii* and *E. nobilii* HSP70 genes are available at NCBI with the accession numbers AY295877 and DQ866998, according to the previous studies [15, 16]. The essential amino acid positions of Hsp70 were reported in previous studies [112, 113]. The consensus amino acids sequence of Hsp70 was according to the previous reports [15, 16].

Phylogenetic analysis

The DNA and amino acid sequences of *Euplotes* pheromones homologous genes were acquired from NCBI, according to the previous work [50], and aligned by MUSCLE v3.8.31 and ClustalW v2.1, respectively [114, 115]. Maximum Likelihood tree based on amino acid sequences was reconstructed by MEGA v7.0.20, using the LG model of amino acid substitution, 500 bootstrap replicates [116, 117].

For phylogenomic analysis by supertree approach, predicted protein sequences of *Euplotes vannus* by us and other 31 ciliates from previous works or transcriptome sequencing by the Marine Microbial Eukaryote Transcriptome Sequencing Project (data available on iMicrobe: http://imicrobe.us/, accession number and gene ID see supplementary information, Table S10) [95, 118-121] were used to generate the concatenated dataset. Maximum Likelihood tree based on the concatenated dataset covering 157 genes was reconstructed by using GPSit v1.0 (relaxed masking, E-value cutoff = 1e-10, sequence identity cutoff = 50%) [58] and RAXML-HPC2 v8.2.9 (on CIPRES Science Gateway, LG model of amino acid substitution + Γ distribution + F, four rate categories, 500 bootstrap replicates) [122]. Trees were visualized by MEGA version 7.0.20 [116].

Additional files

Figure S1. K-mer analysis of *Euplotes vannus* mating types to estimated genome size.

580 **Figure S2.** Genome assembly completeness evaluation of ciliates by BUSCO.

581 **Figure S3.** Venn diagram shows the genes annotated by BLASTX and Interproscan.

582 **Figure S4.** Schematic representation of the exon/intron boundaries with WebLogo in all
583 78661 introns in *E. vannus* mating type EVJ. The GTR and YAG motifs are well conserved.

584 **Figure S5.** A schema illustrates the criteria for detecting +1 frameshifting events. Blue
585 boxes indicate the different BLASTX hits of a CDS region to a same target protein
586 sequence (E-value cutoff = 1e-5). Grey boxes indicate the adjacent region between two
587 BLASTX hits of a CDS region (inner distance cutoff = 10 nt). The brackets above denote
588 the 0-frame codons and the brackets underneath denote the +1-frame codons. Yellow dots
589 denote the nucleotides while the red ones denote the slippery site where frameshifting
590 events occur.

591 **Figure S6.** Sequence alignment of the reverse compliments of the MAC contigs containing
592 Type-II pheromone coding genes in *E. vannus* and *E. crassus*. Blue and red boxes denote
593 the start and stop codon of the coding region of pheromone genes, respectively.

594 **Figure S7.** Sequence alignment of the Type-I pheromone protein sequences in *E. vannus*
595 and *E. crassus*. Identical residues are shadowed in black and similar residues are shaded
596 in grey. Asterisks mark the positions of stop codons. Filled and light arrowheads indicate
597 the extension positions of the pre- and pro-regions, respectively. Red dotes denote the
598 conserved cysteine residues in secreted region. Numbers indicate the progressive amino
599 acid positions in the sequences.

600 **Figure S8.** Sequence alignment of the reverse compliments of the MAC contigs containing
601 Type-I pheromone coding genes in *E. vannus* and *E. crassus*. Blue and red boxes denote
602 the start and stop codon of the coding region of pheromone genes, respectively.

603 **Figure S9.** GBrowse snapshots of genomic and transcriptomic reads mapping on
604 pheromone gene-related chromosomes in different mating types.

605 **Figure S10.** Overall gene expression level in starved or vegetative cells of different mating
606 types.

607 **Figure S11.** Venn diagram shows a large part of mating type-specific transcripts is also
608 starvation induced.

609 **Figure S12.** Species relationship and functional annotation of the mating type-specific and
610 starvation induced transcripts.

611 **Figure S13.** Differential gene expression analysis under temperature, salinity and free
612 ammonia stresses (relative to Figure 5). (A) PCA analysis on gene expression of mating
613 type EVJ under different stresses. (B) Different environmental stresses activated or
614 deactivated different gene groups.

615 **Figure S14.** Sequence alignment of Hsp70 protein sequences.

616 **Table S1.** Mating pattern observed when cultures of two mating types are mixed and
617 genomic and transcriptomic (mRNA) data accessibility of six mating types of *E. vannus*.

618 **Table S2.** Genome assembly information of four mating types of *Euplotes vannus*.

619 **Table S3**. Genomic and transcriptomic reads mapping information.

620 **Table S4**. List of identified ncRNAs.

621 **Table S5.** Annotation information of repeats in the merged genome assembly of *E. vannus*.

622 **Table S6.** Expression and annotation information of *Euplotes vannus* genes.

623 **Table S7.** Homologs of mating-type loci in each mating type.

624 **Table S8.** Homologous search results by BLASTN reveal the relationship between coding
625 regions of four pheromone genes in MAC genome and the corresponding MDS regions in
626 MIC genome of *E. vannus*.

627 **Table S9**. PCR primers for genotyping of Type-II pheromone genes in *E. vannus* and
628 determine mating types.

629 **Table S10.** Information of accession of genome/transcriptome assemblies of 32 ciliates.

630

631 **Abbreviations**

632 Ev: *Euplotes vannus*; Ec: *Euplotes crassus*; Eo: *Euplotes octocarinatus*; En: *Euplotes*
633 *nobilii*; Er: *Euplotes raikovi*; IES: internal eliminated sequence; MAC: macronucleus; MIC:
634 micronucleus; MDS: macronucleus destined sequence; ML: maximum likelihood; MTD:
635 mating type determination; PRF: programmed ribosomal frameshifting.

Acknowledgements

The authors would like to thank the following people for assistance with this study: Tengteng Zhang and Ruitao Gong (Ocean University of China, China), for the assistance of experimental verification; Dr. Fengbiao Mao (University of Michigan, USA), for the advice on data visualization; Dr. Estienne Swart (Max Planck Institute, Germany) for the advice on the preparation of the manuscript.

Funding

This research was funded by the Aoshan Science and Technology Innovation Program of the Qingdao National Laboratory for Marine Science and Technology, Natural Science Foundation of China (project No. 31772428), Young Elite Scientists Sponsorship Program by CAST (2017QNRC001) and the Fundamental Research Funds for the Central Universities (201841013 and 201762017). Research reported in this publication was also supported by the grants of the National Institutes of Health (award number P40OD010964) and the National Science Foundation (grant No. 1158346) to Naomi A. Stover and two grants to Laura A. Katz (NSF DEB-1541511 and NIH 1R15GM113177-01). The content is solely the responsibility of the authors and does not necessarily represent the official views of the National Institutes of Health. Any opinions, findings, and conclusions or recommendations expressed in this material are those of the author(s) and do not necessarily reflect the views of the National Science Foundation.

Availability of data and materials

Euplotes vannus MAC genome assembly and gene annotation data including coding regions and predicted protein sequences are available at *Euplotes vannus* DB (EVDB, http://evan.ciliate.org).

Authors' contributions

XC and FG conceived the study; YHJ and WBZ provided the biological materials; XC designed the experiments; YHJ performed the experiments; XC performed computational and experimental analysis for all figures and tables; XC, FG, CL, LK and WS interpreted the data; TK and NS constructed the genome database website; XC wrote the paper with contribution from all authors. All authors read and approved the final manuscript.

Ethics approval and consent to participate

Not applicable.

Consent for publication

Not applicable.

Competing interests

The authors declare that they have no competing interests.

References

1. Lynn D: **Ciliates.** In *Encyclopedia of Microbiology (Third Edition).* Edited by Schaechter M. Oxford: Academic Press; 2009: 578-592
2. Xu H, Zhang W, Jiang Y, Yang EJ: **Use of biofilm-dwelling ciliate communities to determine environmental quality status of coastal waters.** *Sci Total Environ* 2014, **470:**511-518.
3. Jiang L, Morin PJ: **Temperature-dependent interactions explain unexpected responses to environmental warming in communities of competitors.** *J Anim Ecol* 2004, **73:**569-576.
4. Gong J, Song W, Warren A: **Periphytic ciliate colonization: annual cycle and responses to environmental conditions.** *Aquat Microb Ecol* 2005, **39:**159-170.
5. Stoeck T, Kochems R, Forster D, Lejzerowicz F, Pawlowski J: **Metabarcoding of benthic ciliate communities shows high potential for environmental monitoring in salmon aquaculture.** *Ecological Indicators* 2018, **85:**153-164.
6. Yeomans W, Chubb J, Sweeting R: **Use of protozoan communities for pollution monitoring.** *Parassitologia* 1997, **39:**201-212.
7. Gutiérrez JC, Martín-González A, Díaz S, Ortega R: **Ciliates as a potential source of cellular and molecular biomarkers/biosensors for heavy metal pollution.** *Eur J Protistol* 2003, **39:**461-467.

8. Jiang Y, Xu H, Hu X, Zhu M, Al-Rasheid KA, Warren A: **An approach to analyzing spatial patterns of planktonic ciliate communities for monitoring water quality in Jiaozhou Bay, northern China.** *Mar Pollut Bull* 2011, **62:**227-235.
9. Borror AC: **Spatial distribution of marine ciliates: Micro-Ecologic and Biogeographic aspects of Protozoan Ecology.** *J Eukaryot Microbiol* 1980, **27:**10-13.
10. Foissner W: **Biogeography and dispersal of micro-organisms: a review emphasizing protists.** *Acta Protozool* 2006, **45:**111-136.
11. Petz W, Valbonesi A, Schiftner U, Quesada A, Cynan Ellis-Evans J: **Ciliate biogeography in Antarctic and Arctic freshwater ecosystems: endemism or global distribution of species?** *Fems Microbiol Ecol* 2007, **59:**396-408.
12. Foissner W, Chao A, Katz LA: **Diversity and geographic distribution of ciliates (Protista: Ciliophora).** *Biodivers Conserv* 2008, **17:**345-363.
13. Liu W, Jiang J, Xu Y, Pan X, Qu Z, Luo X, El-Serehy HA, Warren A, Ma H, Pan H: **Diversity of free-living marine ciliates (Alveolata, Ciliophora): faunal studies in coastal waters of China during the years 2011-2016.** *Eur J Protistol* 2017, **61:**424-438.
14. La Terza A, Papa G, Miceli C, Luporini P: **Divergence between two Antarctic species of the ciliate *Euplotes*, *E. focardii* and *E. nobilii*, in the expression of heat-shock protein 70 genes.** *Mol Ecol* 2001, **10:**1061-1067.
15. La Terza A, Miceli C, Luporini P: **The gene for the heat-shock protein 70 of *Euplotes focardii*, an Antarctic psychrophilic ciliate.** *Antarct Sci* 2004, **16:**23-28.
16. La Terza A, Passini V, Barchetta S, Luporini P: **Adaptive evolution of the heat-shock response in the Antarctic psychrophilic ciliate, *Euplotes focardii*: hints from a comparative determination of the hsp70 gene structure.** *Antarct Sci* 2007, **19:**239-244.
17. Clark MS, Peck LS: **HSP70 heat shock proteins and environmental stress in Antarctic marine organisms: a mini-review.** *Marine genomics* 2009, **2:**11-18.
18. Luo X, Gao F, Yi Z, Pan Y, Al-Farraj SA, Warren A: **Taxonomy and molecular phylogeny of two new brackish hypotrichous ciliates, with the establishment of a new genus (Ciliophora, Spirotrichea).** *Zool J Linn Soc-lond* 2017, **179:**475-491.
19. Yan Y, Rogers AJ, Gao F, Katz LA: **Unusual features of non-dividing somatic macronuclei in the ciliate class Karyorelictea.** *Eur J Protistol* 2017, **61:**399-408.
20. Wang C, Zhang T, Wang Y, Katz LA, Gao F, Song W: **Disentangling sources of variation in SSU rDNA sequences from single cell analyses of ciliates: impact of copy number variation and experimental error.** *Proc R Soc B* 2017, **284:**20170425.
21. Xiong J, Gao S, Dui W, Yang W, Chen X, Taverna SD, Pearlman RE, Ashlock W, Miao W, Liu Y: **Dissecting relative contributions of cis- and trans-determinants to nucleosome distribution by comparing *Tetrahymena* macronuclear and micronuclear chromatin.** *Nucleic Acids Res* 2016, **44:**10091-10105.
22. Wang Y, Chen X, Sheng Y, Liu Y, Gao S: **N6-adenine DNA methylation is associated with the linker DNA of H2A. Z-containing well-positioned nucleosomes in Pol II-transcribed genes in *Tetrahymena*.** *Nucleic Acids Res* 2017, **45:**11594-11606.
23. Wang Y, Wang Y, Sheng Y, Huang J, Chen X, AL-Rasheid KA, Gao S: **A comparative study of genome organization and epigenetic mechanisms in model ciliates, with an emphasis on *Tetrahymena*, *Paramecium* and *Oxytricha*.** *Eur J Protistol* 2017, **61:**376-387.
24. Dhanker R, Kumar R, Tseng L-C, Hwang J-S: **Ciliate (*Euplotes* sp.) predation by *Pseudodiaptomus annandalei* (Copepoda: Calanoida) and the effects of mono-algal and pluri-algal diets.** *Zool Stud* 2013, **52:**34.
25. Kuhlmann H-W: **Escape response of *Euplotes octocarinatus* to turbellarian predators.** *Archiv für Protistenkunde* 1994, **144:**163-171.
26. Kuhlmann H-W, Heckmann K: **Predation risk of typical ovoid and 'winged' morphs of *Euplotes* (Protozoa, Ciliophora).** *Hydrobiologia* 1994, **284:**219-227.

27. Kusch J: **Behavioural and morphological changes in ciliates induced by the predator *Amoeba proteus*.** *Oecologia* 1993, **96:**354-359.
28. Kusch J: **Adaptation of inducible defense in *Euplotes daidaleos* (Ciliophora) to predation risks by various predators.** *Microb Ecol* 1995, **30:**79-88.
29. Kusch J: **Induction of defensive morphological changes in ciliates.** *Oecologia* 1993, **94:**571-575.
30. Kusch J, Kuhlmann HW: **Cost of Stenostomum-induced morphological defence in the ciliate *Euplotes octocarinatus*.** *Arch Hydrobiol* 1994, **130:**257-267.
31. Wiąckowski K, Szkarłat M: **Effects of food availability on predator-induced morphological defence in the ciliate *Euplotes octocarinatus* (Protista).** *Hydrobiologia* 1996, **321:**47-52.
32. Jerka-Dziadosz M, Dosche C, Kuhlmann HW, Heckmann K: **Signal-induced reorganization of the microtubular cytoskeleton in the ciliated protozoon *Euplotes octocarinatus*.** *J Cell Sci* 1987, **87:**555-564.
33. Hadjivasiliou Z, Iwasa Y, Pomiankowski A: **Cell-cell signalling in sexual chemotaxis: a basis for gametic differentiation, mating types and sexes.** *J R Soc Interface* 2015, **12:**20150342.
34. Persoone G, Uyttersprot G: **The influence of inorganic and organic pollutants on the rate of reproduction of a marine hypotrichous ciliate: *Euplotes vannus* Muller.** *Revue Internationale d'Oceanographie Medicale* 1975, **37:**125-152.
35. Trielli F, Amaroli A, Sifredi F, Marchi B, Falugi C, Corrado MU: **Effects of xenobiotic compounds on the cell activities of *Euplotes crassus*, a single-cell eukaryotic test organism for the study of the pollution of marine sediments.** *Aquat Toxicol* 2007, **83:**272-283.
36. Xu H, Song W, Warren A: **An investigation of the tolerance to ammonia of the marine ciliate *Euplotes vannus* (Protozoa, Ciliophora).** *Hydrobiologia* 2004, **519:**189-195.
37. Day JG, Gong Y, Hu Q: **Microzooplanktonic grazers - A potentially devastating threat to the commercial success of microalgal mass culture.** *Algal Research* 2017, **27:**356-365.
38. Walton BM, Gates MA, Kloos A, Fisher J: **Intraspecific variability in the thermal dependence of locomotion, population growth, and mating in the ciliated protist *Euplotes vannus*.** *Physiol Zool* 1995, **68:**98-113.
39. Wang R, Xiong J, Wang W, Miao W, Liang A: **High frequency of +1 programmed ribosomal frameshifting in *Euplotes octocarinatus*.** *Sci Rep* 2016, **6:**21139.
40. Orias E, Singh DP, Meyer E: **Genetics and Epigenetics of mating type determination in *Paramecium* and *Tetrahymena*.** *Annu Rev Microbiol* 2017, **71:**133-156.
41. Singh DP, Saudemont B, Guglielmi G, Arnaiz O, Goût J-F, Prajer M, Potekhin A, Przybòs E, Aubusson-Fleury A, Bhullar S: **Genome-defence small RNAs exapted for epigenetic mating-type inheritance.** *Nature* 2014, **509:**447.
42. Cervantes MD, Hamilton EP, Xiong J, Lawson MJ, Yuan D, Hadjithomas M, Miao W, Orias E: **Selecting one of several mating types through gene segment joining and deletion in Tetrahymena thermophila.** *PLoS biology* 2013, **11:**e1001518.
43. Kimball R: **The nature and inheritance of mating types in *Euplotes patella*.** *Genetics* 1942, **27:**269.
44. Nanney D, Caughey PA, Tefankjian A: **The genetic control of mating type potentialities in *Tetrahymena pyriformis*.** *Genetics* 1955, **40:**668.
45. Siegel R, Larison L: **The genic control of mating types in *Paramecium bursaria*.** *Proc Natl Acad Sci* 1960, **46:**344-349.
46. Akada R: **Mating types and mating-inducing factors (gamones) in the ciliate *Euplotes patella* syngen 2.** *Genet Res* 1985, **46:**125-132.

47. Dini F, Luporini P: **Mating-type polymorphic variation in *Euplotes minuta* (Ciliophora: Hypotrichida).** *The Journal of protozoology* 1985, **32:**111-117.
48. Heckmann K, Kuhlmann HW: **Mating types and mating inducing substances in *Euplotes octocarinatus*.** *J Exp Zool* 1986, **237:**87-96.
49. Alimenti C, Vallesi A, Federici S, Di Giuseppe G, Fernando D, Carratore V, Luporini P: **Isolation and structural characterization of two water-borne pheromones from *Euplotes crassus*, a ciliate commonly known to carry membrane-bound pheromones.** *J Eukaryot Microbiol* 2011, **58:**234-241.
50. Vallesi A, Alimenti C, Federici S, Di Giuseppe G, Dini F, Guella G, Luporini P: **Evidence for gene duplication and allelic codominance (not hierarchical dominance) at the mating-type locus of the ciliate, *Euplotes crassus*.** *J Eukaryot Microbiol* 2014, **61:**620-629.
51. Di Giuseppe G, Erra F, Dini F, Alimenti C, Vallesi A, Pedrini B, Wüthrich K, Luporini P: **Antarctic and Arctic populations of the ciliate *Euplotes nobilii* show common pheromone-mediated cell-cell signaling and cross-mating.** *Proc Natl Acad Sci* 2011, **108:**3181-3186.
52. Vallesi A, Alimenti C, Luporini P: **Ciliate pheromones: primordial self-/nonself-recognition signals.** In *Lessons in Immunity.* Elsevier; 2016: 1-16
53. Dini F, Nyberg D: **Sex in ciliates.** In *Adv Microb Ecol.* Springer; 1993: 85-153
54. Heckmann K: **Experimentelle Untersuchungen an *Euplotes crassus*.** *Zeitschrift für Vererbungslehre* 1964, **95:**114-124.
55. Nobili R, Luporini P, Dini F: **Breeding systems, species relationships and evolutionary trends in some marine species of Euplotidae (Hypotrichida Ciliata).** *Marine organisms: genetics, ecology, and evolution Plenum, New York* 1978**:**591-616.
56. Kim B-M, Rhee J-S, Choi I-Y, Lee Y-M: **Transcriptional profiling of antioxidant defense system and heat shock protein (Hsp) families in the cadmium- and copper-exposed marine ciliate *Euplotes crassus*.** *Genes & Genomics* 2018, **40:**85-98.
57. Kim S-J, Kim J-H, Ju S-J: **Adaptation responses of individuals to environmental changes in the ciliate *Euplotes crassus*.** *Ocean Science Journal* 2017, **52:**127-138.
58. Chen X, Wang Y, Sheng Y, Warren A, Gao S: **GPSit: An automated method for evolutionary analysis of nonculturable ciliated microeukaryotes.** *Mol Ecol Resour* 2018, **4:**1-14.
59. Acorn AR, Clark KF, Jones S, Després BM, Munro S, Cawthorn RJ, Greenwood SJ: **Analysis of expressed sequence tags (ESTs) and gene expression changes under different growth conditions for the ciliate *Anophryoides haemophila*, the causative agent of bumper car disease in the American lobster (*Homarus americanus*).** *J Invertebr Pathol* 2011, **107:**146-154.
60. Cheung P, Nigrelli R, Ruggieri G: **Studies on the morphology of *Uronema marinum* Dujardin (Ciliatea: Uronematidae) with a description of the histopathology of the infection in marine fishes.** *J Fish Dis* 1980, **3:**295-303.
61. Dragesco A, Dragesco J, Coste F, Gasc C, Romestand B, Raymond J-C, Bouix G: ***Philasterides dicentrarchi*, n. sp.,(Ciliophora, Scuticociliatida), a histophagous opportunistic parasite of *Dicentrarchus labrax* (Linnaeus, 1758), a reared marine fish.** *Eur J Protistol* 1995, **31:**327-340.
62. Iglesias R, Paramá A, Alvarez M, Leiro J, Fernández J, Sanmartín M: ***Philasterides dicentrarchi* (Ciliophora, Scuticociliatida) as the causative agent of scuticociliatosis in farmed turbot *Scophthalmus maximus* in Galicia (NW Spain).** *Dis Aquat Organ* 2001, **46:**47-55.
63. Munday B, O'Donoghue P, Watts M, Rough K, Hawkesford T: **Fatal encephalitis due to the scuticociliate *Uronema nigricans* in sea-caged, southern bluefin tuna *Thunnus maccoyii*.** *Dis Aquat Organ* 1997, **30:**17-25.

64. Swart EC, Serra V, Petroni G, Nowacki M: **Genetic codes with no dedicated stop codon: context-dependent translation termination.** *Cell* 2016, **166:**691-702.
65. Heaphy SM, Mariotti M, Gladyshev VN, Atkins JF, Baranov PV: **Novel ciliate genetic code variants including the reassignment of all three stop codons to sense codons in *Condylostoma magnum*.** *Mol Biol Evol* 2016, **33:**2885-2889.
66. Valbonesi A, Ortenzi C, Luporini P: **An integrated study of the species problem in the *Euplotes crassus-minuta-vannus* group.** *J Eukaryot Microbiol* 1988, **35:**38-45.
67. Dobzhansky T: **Speciation as a stage in evolutionary divergence.** *The American Naturalist* 1940, **74:**312-321.
68. Zhao Y, Yi Z, Warren A, Song WB: **Species delimitation for the molecular taxonomy and ecology of the widely distributed microbial eukaryote genus *Euplotes* (Alveolata, Ciliophora).** *Proc R Soc B* 2018, **285:**20172159.
69. Brown L, Mronga S, Bradshaw R, Ortenzi C, Luporini P, Wüthrich K: **Nuclear magnetic resonance solution structure of the pheromone Er-10 from the ciliated protozoan *Euplotes raikovi*.** *J Mol Biol* 1993, **231:**800-816.
70. Ottiger M, Szyperski T, Luginbühl P, Ortenzi C, Luporini P, Bradshaw R, Wüthrich K: **The NMR solution structure of the pheromone Er-2 from the ciliated protozoan *Euplotes raikovi*.** *Protein Sci* 1994, **3:**1515-1526.
71. Mronga S, Luginbühl P, Brown L, Ortenzi C, Luporini P, Bradshaw R, Wüthrich K: **The NMR solution structure of the pheromone Er-1 from the ciliated protozoan *Euplotes raikovi*.** *Protein Sci* 1994, **3:**1527-1536.
72. Luginbühl P, Ottiger M, Mronga S, WÜthrich K: **Structure comparison of the pheromones Er-1, Er-10, and Er-2 from *Euplotes raikovi*.** *Protein Sci* 1994, **3:**1537-1546.
73. Weiss MS, Anderson DH, Raffioni S, Bradshaw RA, Ortenzi C, Luporini P, Eisenberg D: **A cooperative model for receptor recognition and cell adhesion: evidence from the molecular packing in the 1.6-A crystal structure of the pheromone Er-1 from the ciliated protozoan *Euplotes raikovi*.** *Proc Natl Acad Sci* 1995, **92:**10172-10176.
74. Liua A, Luginbühla P, Zerbea O, Ortenzib C, Luporinib P, Wüthrichа K: **NMR structure of the pheromone Er-22 from *Euplotes raikovi*.** *J Biomol NMR* 2001, **19:**75-78.
75. Zahn R, Damberger F, Ortenzi C, Luporini P, Wüthrich K: **NMR structure of the *Euplotes raikovi* pheromone Er-23 and identification of its five disulfide bonds.** *J Mol Biol* 2001, **313:**923-931.
76. Vallesi A, Alimenti C, Pedrini B, Di Giuseppe G, Dini F, Wüthrich K, Luporini P: **Coding genes and molecular structures of the diffusible signalling proteins (pheromones) of the polar ciliate, *Euplotes nobilii*.** *Marine genomics* 2012, **8:**9-13.
77. Pedrini B, Placzek WJ, Koculi E, Alimenti C, LaTerza A, Luporini P, Wüthrich K: **Cold-adaptation in sea-water-borne signal proteins: sequence and NMR structure of the pheromone En-6 from the Antarctic ciliate *Euplotes nobilii*.** *J Mol Biol* 2007, **372:**277-286.
78. Placzek WJ, Etezady-Esfarjani T, Herrmann T, Pedrini B, Peti W, Alimenti C, Luporini P, Wüthrich K: **Cold-adapted signal proteins: NMR structures of pheromones from the antarctic ciliate *Euplotes nobilii*.** *Iubmb Life* 2007, **59:**578-585.
79. Schulze Dieckhoff H, Freiburg M, Heckmann K: **The isolation of gamones 3 and 4 of *Euplotes octocarinatus*.** *The FEBS Journal* 1987, **168:**89-94.
80. Brünen-Nieweier C, Weiligmann JC, Hansen B, Kuhlmann H-W, Möllenbeck M, Heckmann K: **The pheromones and pheromone genes of new stocks of the *Euplotes octocarinatus* species complex.** *Eur J Protistol* 1998, **34:**124-132.
81. Möllenbeck M, Heckmann K: **Characterization of two genes encoding a fifth so far unknown pheromone of *Euplotes octocarinatus*.** *Eur J Protistol* 1999, **35:**225-230.

82. Kuhlmann H-W, Brünen-Nieweler C, Heckmann K: **Pheromones of the ciliate *Euplotes octocarinatus* not only induce conjugation but also function as chemoattractants.** *J Exp Zool* 1997, **277:**38-48.
83. Chen X, Ma H-G, Al-Rasheid KA, Miao M: **Molecular data suggests the ciliate *Mesodinium* (Protista: Ciliophora) might represent an undescribed taxon at class level.** *Zoological Systematics* 2015, **1:**002.
84. Kobayashi N, McENTEE K: **Identification of cis and trans components of a novel heat shock stress regulatory pathway in *Saccharomyces cerevisiae*.** *Mol Cell Biol* 1993, **13:**248-256.
85. Fernandes M: **Structure and regulation of heat shock gene promoters.** *The biology of heat shock proteins and molecular chaperones* 1994**:**375-393.
86. Ruis H, Schüller C: **Stress signaling in yeast.** *Bioessays* 1995, **17:**959-965.
87. Nurk S, Bankevich A, Antipov D, Gurevich AA, Korobeynikov A, Lapidus A, Prjibelski AD, Pyshkin A, Sirotkin A, Sirotkin Y: **Assembling single-cell genomes and mini-metagenomes from chimeric MDA products.** *J Comput Biol* 2013, **20:**714-737.
88. Bankevich A, Nurk S, Antipov D, Gurevich AA, Dvorkin M, Kulikov AS, Lesin VM, Nikolenko SI, Pham S, Prjibelski AD: **SPAdes: a new genome assembly algorithm and its applications to single-cell sequencing.** *J Comput Biol* 2012, **19:**455-477.
89. Fu L, Niu B, Zhu Z, Wu S, Li W: **CD-HIT: accelerated for clustering the next-generation sequencing data.** *Bioinformatics* 2012, **28:**3150-3152.
90. Huang X, Madan A: **CAP3: A DNA sequence assembly program.** *Genome Res* 1999, **9:**868-877.
91. Simao FA, Waterhouse RM, Ioannidis P, Kriventseva EV, Zdobnov EM: **BUSCO: assessing genome assembly and annotation completeness with single-copy orthologs.** *Bioinformatics* 2015, **31:**3210-3212.
92. Kim D, Langmead B, Salzberg SL: **HISAT: a fast spliced aligner with low memory requirements.** *Nat Methods* 2015, **12:**357-360.
93. Stein LD: **Using GBrowse 2.0 to visualize and share next-generation sequence data.** *Brief Bioinform* 2013, **14:**162-171.
94. Lobanov AV, Heaphy SM, Turanov AA, Gerashchenko MV, Pucciarelli S, Devaraj RR, Xie F, Petyuk VA, Smith RD, Klobutcher LA, et al: **Position-dependent termination and widespread obligatory frameshifting in *Euplotes* translation.** *Nat Struct Mol Biol* 2017, **24:**61-68.
95. Wang R, Miao W, Wang W, Xiong J, Liang A: **EOGD: the *Euplotes octocarinatus* genome database.** *BMC Genomics* 2018, **19:**63.
96. Swart EC, Bracht JR, Magrini V, Minx P, Chen X, Zhou Y, Khurana JS, Goldman AD, Nowacki M, Schotanus K, et al: **The *Oxytricha trifallax* macronuclear genome: a complex eukaryotic genome with 16,000 tiny chromosomes.** *PLoS Biol* 2013, **11:**29.
97. Tarailo-Graovac M, Chen N: **Using RepeatMasker to identify repetitive elements in genomic sequences.** *Curr Protoc Bioinformatics* 2009, **4:**4-10.
98. Stanke M, Tzvetkova A, Morgenstern B: **AUGUSTUS at EGASP: using EST, protein and genomic alignments for improved gene prediction in the human genome.** *Genome Biology* 2006, **7:**1.
99. Lowe TM, Eddy SR: **tRNAscan-SE: a program for improved detection of transfer RNA genes in genomic sequence.** *Nucleic Acids Res* 1997, **25:**955-964.
100. Burge SW, Daub J, Eberhardt R, Tate J, Barquist L, Nawrocki EP, Eddy SR, Gardner PP, Bateman A: **Rfam 11.0: 10 years of RNA families.** *Nucleic Acids Res* 2013, **41:**3.
101. Pertea M, Pertea GM, Antonescu CM, Chang TC, Mendell JT, Salzberg SL: **StringTie enables improved reconstruction of a transcriptome from RNA-seq reads.** *Nat Biotechnol* 2015, **33:**290-295.

102. Jones P, Binns D, Chang HY, Fraser M, Li W, McAnulla C, McWilliam H, Maslen J, Mitchell A, Nuka G, et al: **InterProScan 5: genome-scale protein function classification.** *Bioinformatics* 2014, **30:**1236-1240.
103. Camacho C, Coulouris G, Avagyan V, Ma N, Papadopoulos J, Bealer K, Madden TL: **BLAST+: architecture and applications.** *BMC Bioinformatics* 2009, **10:**1471-2105.
104. Crooks GE, Hon G, Chandonia JM, Brenner SE: **WebLogo: a sequence logo generator.** *Genome Res* 2004, **14:**1188-1190.
105. Liao Y, Smyth GK, Shi W: **featureCounts: an efficient general purpose program for assigning sequence reads to genomic features.** *Bioinformatics* 2013, **30:**923-930.
106. Frazee AC, Pertea G, Jaffe AE, Langmead B, Salzberg SL, Leek JT: **Ballgown bridges the gap between transcriptome assembly and expression analysis.** *Nat Biotechnol* 2015, **33:**243-246.
107. Love MI, Huber W, Anders S: **Moderated estimation of fold change and dispersion for RNA-seq data with DESeq2.** *Genome Biol* 2014, **15:**014-0550.
108. Langfelder P, Horvath S: **WGCNA: an R package for weighted correlation network analysis.** *BMC Bioinformatics* 2008, **9:**559.
109. Maere S, Heymans K, Kuiper M: **BiNGO: a Cytoscape plugin to assess overrepresentation of gene ontology categories in biological networks.** *Bioinformatics* 2005, **21:**3448-3449.
110. Kohl M, Wiese S, Warscheid B: **Cytoscape: software for visualization and analysis of biological networks.** *Methods Mol Biol* 2011, **696:**291-303.
111. Wickham H: *ggplot2: elegant graphics for data analysis.* Springer; 2016.
112. Sriram M, Osipiuk J, Freeman B, Morimoto R, Joachimiak A: **Human Hsp70 molecular chaperone binds two calcium ions within the ATPase domain.** *Structure* 1997, **5:**403-414.
113. Morshauser RC, Hu W, Wang H, Pang Y, Flynn GC, Zuiderweg ER: **High-resolution solution structure of the 18 kDa substrate-binding domain of the mammalian chaperone protein Hsc701.** *J Mol Biol* 1999, **289:**1387-1403.
114. Edgar RC: **MUSCLE: multiple sequence alignment with high accuracy and high throughput.** *Nucleic Acids Res* 2004, **32:**1792-1797.
115. Chenna R, Sugawara H, Koike T, Lopez R, Gibson TJ, Higgins DG, Thompson JD: **Multiple sequence alignment with the Clustal series of programs.** *Nucleic Acids Res* 2003, **31:**3497-3500.
116. Kumar S, Stecher G, Tamura K: **MEGA7: Molecular Evolutionary Genetics Analysis version 7.0 for bigger datasets.** *Mol Biol Evol* 2016, **33:**1870-1874.
117. Le SQ, Gascuel O: **An improved general amino acid replacement matrix.** *Mol Biol Evol* 2008, **25:**1307-1320.
118. Keeling PJ, Burki F, Wilcox HM, Allam B, Allen EE, Amaral-Zettler LA, Armbrust EV, Archibald JM, Bharti AK, Bell CJ, et al: **The Marine Microbial Eukaryote Transcriptome Sequencing Project (MMETSP): illuminating the functional diversity of eukaryotic life in the oceans through transcriptome sequencing.** *PLoS Biol* 2014, **12**.
119. Gentekaki E, Kolisko M, Gong Y, Lynn D: **Phylogenomics solves a long-standing evolutionary puzzle in the ciliate world: The subclass Peritrichia is monophyletic.** *Mol Phylogenet Evol* 2017, **106:**1-5.
120. Aeschlimann SH, Jonsson F, Postberg J, Stover NA, Petera RL, Lipps HJ, Nowacki M, Swart EC: **The draft assembly of the radically organized *Stylonychia lemnae* macronuclear genome.** *Genome Biol Evol* 2014, **6:**1707-1723.
121. Slabodnick MM, Ruby JG, Reiff SB, Swart EC, Gosai S, Prabakaran S, Witkowska E, Larue GE, Fisher S, Freeman RM, Jr., et al: **The macronuclear genome of *Stentor coeruleus* reveals tiny introns in a giant cell.** *Curr Biol* 2017, **27:**569-575.
122. Stamatakis A: **RAxML version 8: a tool for phylogenetic analysis and post-analysis of large phylogenies.** *Bioinformatics* 2014, **30:**1312-1313.

Table 1. MAC genome assembly and transcriptome-improved gene annotation of *Euplotes vannus* in comparison with that of other euplotids.

	E. vannus	***E. crassus***	***E. octocarinatus***
Genome size (Mb)	85.1	58.6	88.9
%GC	37.0	38.7	28.2
Contig #	38245	56587	41980
Contig N50 (bp)	2685	1581	2947
2-telomere contig #	25519	13783	29532
1-telomere contig #	7835	20646	4842
0-telomere contig #	4890	22158	7606
2-telomere contig percentage (%)	66.7	24.4	70.3
Genome size (with telomere) (Mb)	52.5	44.9	83.1
Scaffold (with telomere) #	33354	34429	34374
%Scaffold (with telomere)	87.2	60.8	81.9
Scaffold N50 (bp)	2714	1830	2999
Gene #	32755	-	29076
Exon #	175735	-	96843
Transcript #	43040	-	29076

Table 2. MIC genome assembly information of *Euplotes vannus* and recognition of MDS-containing contigs and those contain multiple MDSs.

MIC genome	Total	With MDS	Multi-MDS
Genome size (Mb)	120.0	49.8	31.8
%GC	36.0	35.7	35.9
Contig #	104988	13140	5166
Contig N50 (bp)	1953	5597	7718

Figure captions

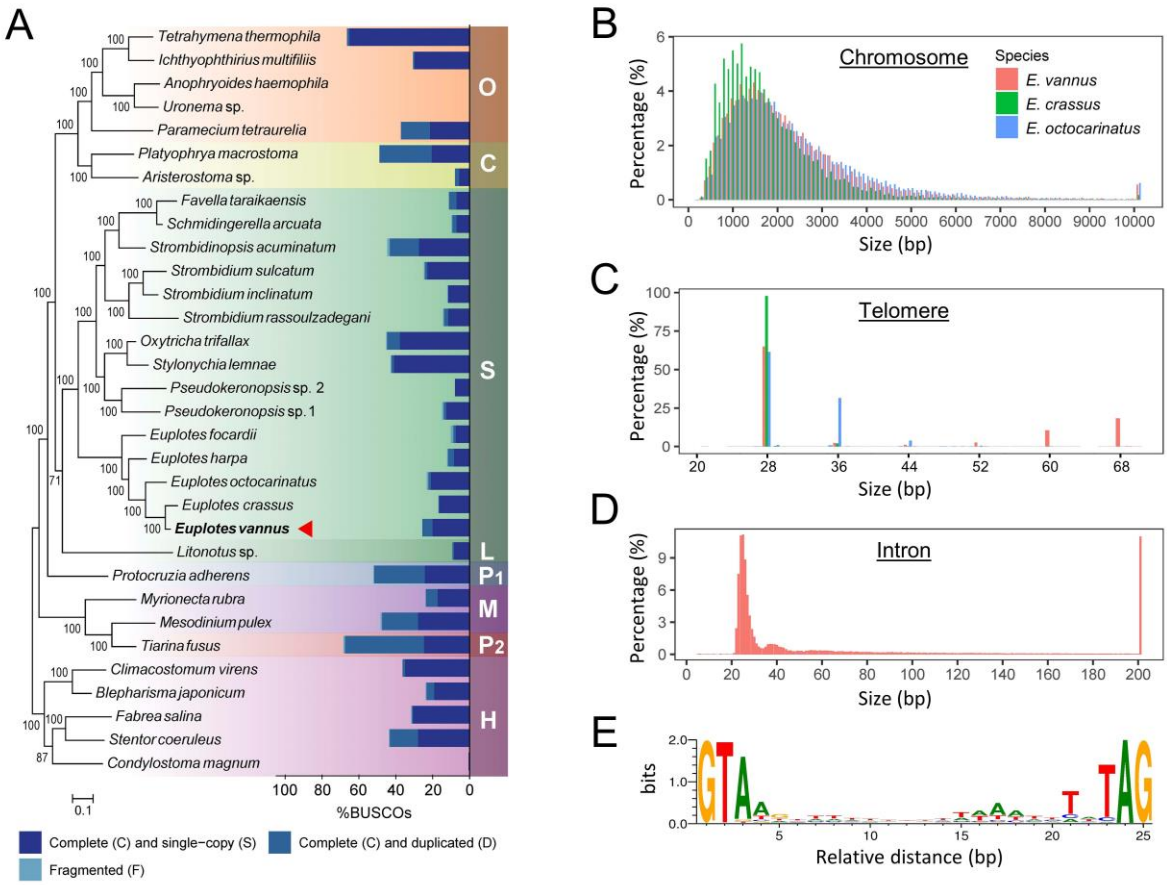

Figure 1. Genome assembly of *E. vannus*. (A) Maximum likelihood phylogenetic tree by supermatrix approach and assembly completeness evaluation of ciliate genomes/transcriptomes by BUSCO. Dark blue blocks represent the percentage of complete and single-copy genes among protists, and the steel-blue blocks represent that of complete and duplicated genes in each species. Genomic data of *Euplotes vannus* sequenced in the current work is marked by the red triangle. S: class Spirotrichea. L: class Litostomatea. O: class Oligohymenophorea. C: class Colpodea. P1: class Protocruzia. M: class Mesodiniea. P2: class Prostomatea. H: class Heterotrichea. The scale bar corresponds to 10 substitutions per 100 nucleotide positions. (B) Size distribution of 2-telomere scaffolds of *E. vannus*, *E. crassus* and *E. octocarinatus*. (C) Size distribution of telomeres of *E. vannus*, *E. crassus* and *E. octocarinatus*. (D) Size distribution of introns in *E. vannus* mating type EVJ. (E) Sequence motif of 8792 tiny introns with the size of 25 nt. Weblogo was generated and normalized to neutral base frequencies in intergenic regions.

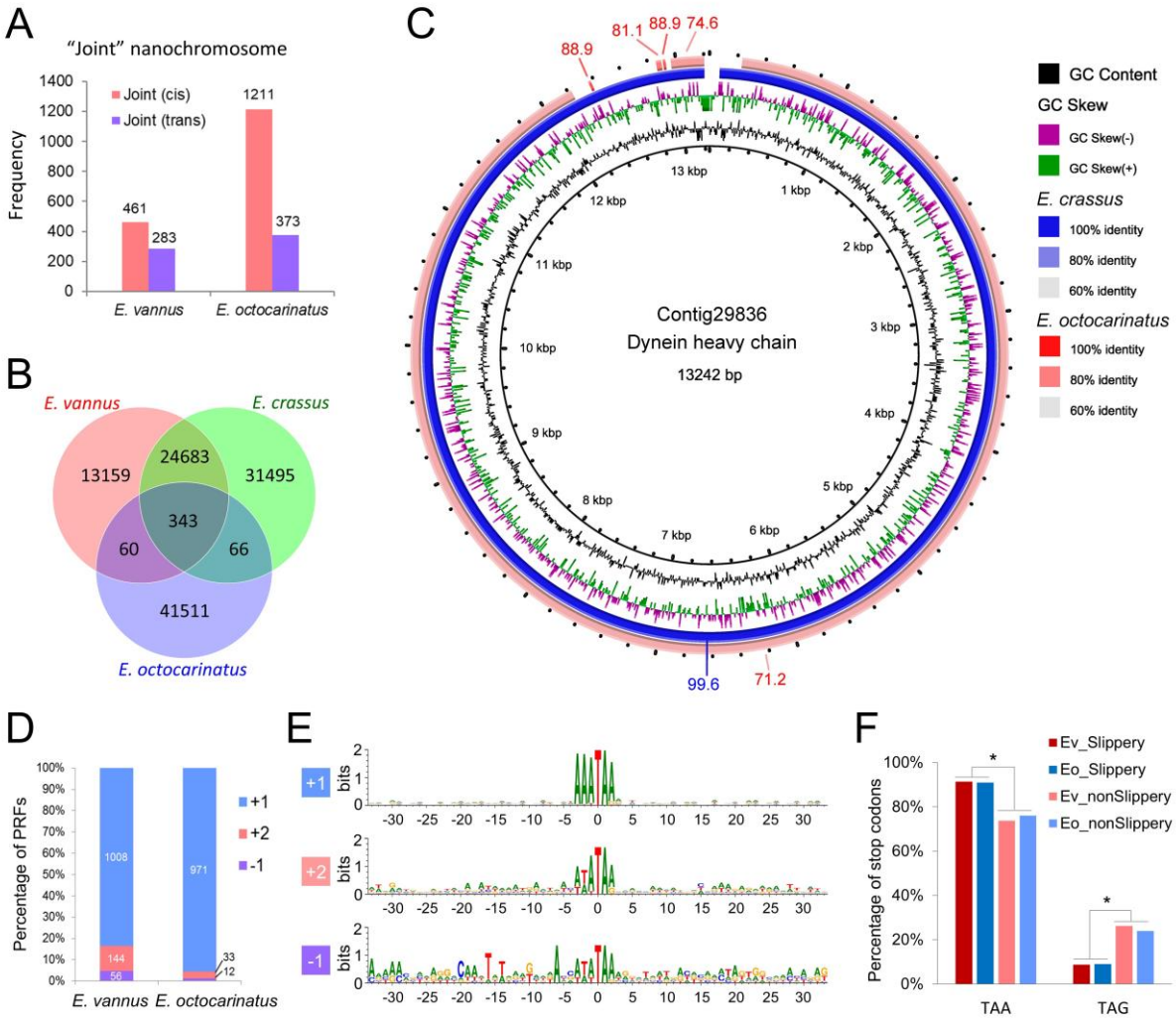

Figure 2. Evolution and synteny/comparative genomic analyses. (A) "Joint" nanochromosome detection in *E. vannus* and *E. octocarinatus*. Red bars denote the frequency of joint nanochromosomes containing genes in a same transcription direction (cis) and purple bars denote that of joint nanochromosomes containing genes in opposite transcription directions (trans). (B) Closely related contigs among three euplotids. (C) Homologous comparison of the contigs containing dynein heavy chain coding gene among *E. vannus* (as reference), *E. crassus* (blue) and *E. octocarinatus* (red). (D) Frameshifting detection & comparison with *E. octocarinatus*. (E) Conserved sequence motif associated with frameshift sites. Sizes of letters denote information content, or sequence conservation, at each position. The analysis is based on the alignment of 30 bp upstream and downstream the frameshifting motif from 1236 predicted +1 frameshifting events that involves stop codon TAA or TAG. Note the canonical motif 5'-AAA-TAR-3' (R = A or G) in +1 PRF and noncanonical motif 5'-WWW-TAR-3' (W = A or T) in +2 and -1 PRF. (F) Stop codon usage in slippery and non-slippery transcripts of *E. vannus* (Ev) and *E. octocarinatus* (Eo). Asterisks denote the significant difference ($p < 0.01$).

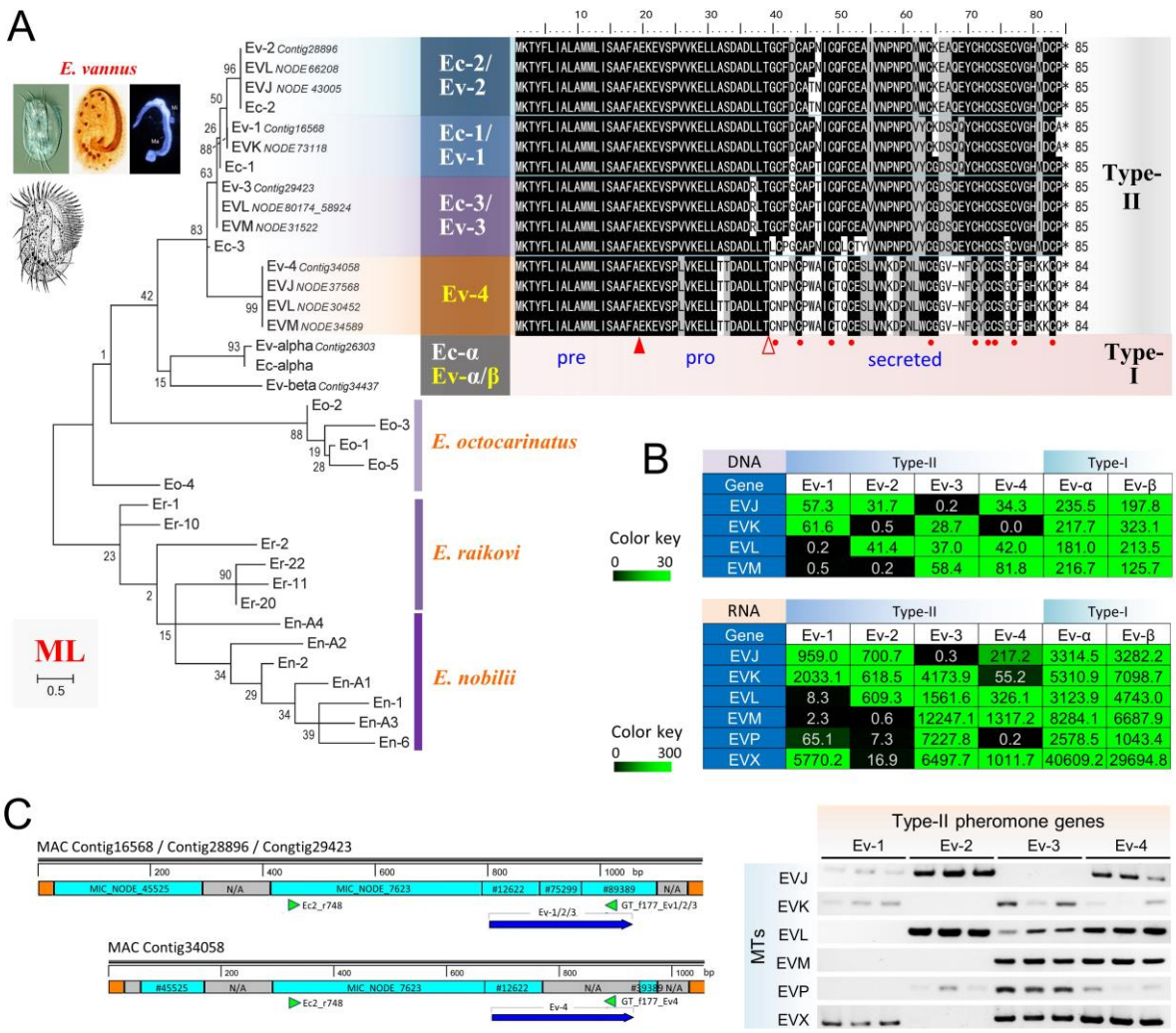

Figure 3. Genomic investigation revealed new pheromone loci Ev-4 and Ev-beta and a mating type-specific combination of these loci in *E. vannus*. (A) Phylogenetic analysis of *Euplotes* pheromones and sequence alignment of Type-II pheromones of *E. vannus* and *E. crassus*. Identical residues are shadowed in black and similar residues are shaded in grey. Asterisks mark the positions of stop codons. Filled and light arrowheads indicate the extension positions of the pre- and pro-regions, respectively. Red dotes denote the 10 conserved cysteine residues in secreted region. Numbers indicate the progressive amino acid positions in the sequences. (B) Chromatin and gene expression profiling based on the RPKM of pheromone loci in each mating type of *E. vannus* by genome and transcriptome sequencing. The tables are colored by RPKM values. (C) The primer design (left) and PCR amplification results (right) of *E. vannus* Type-II pheromone genes. Boxes in orange, blue and grey denote the telomeres of the MAC contigs containing the pheromone genes, the MDS regions and regions those loci in MIC genome still unknown (N/A), respectively. Arrow heads in green denote the positions of the primers. Arrows in blue denote the coding regions of pheromone genes. PCR amplifications of each pheromone gene in each mating type are conducted with three biological replicates.

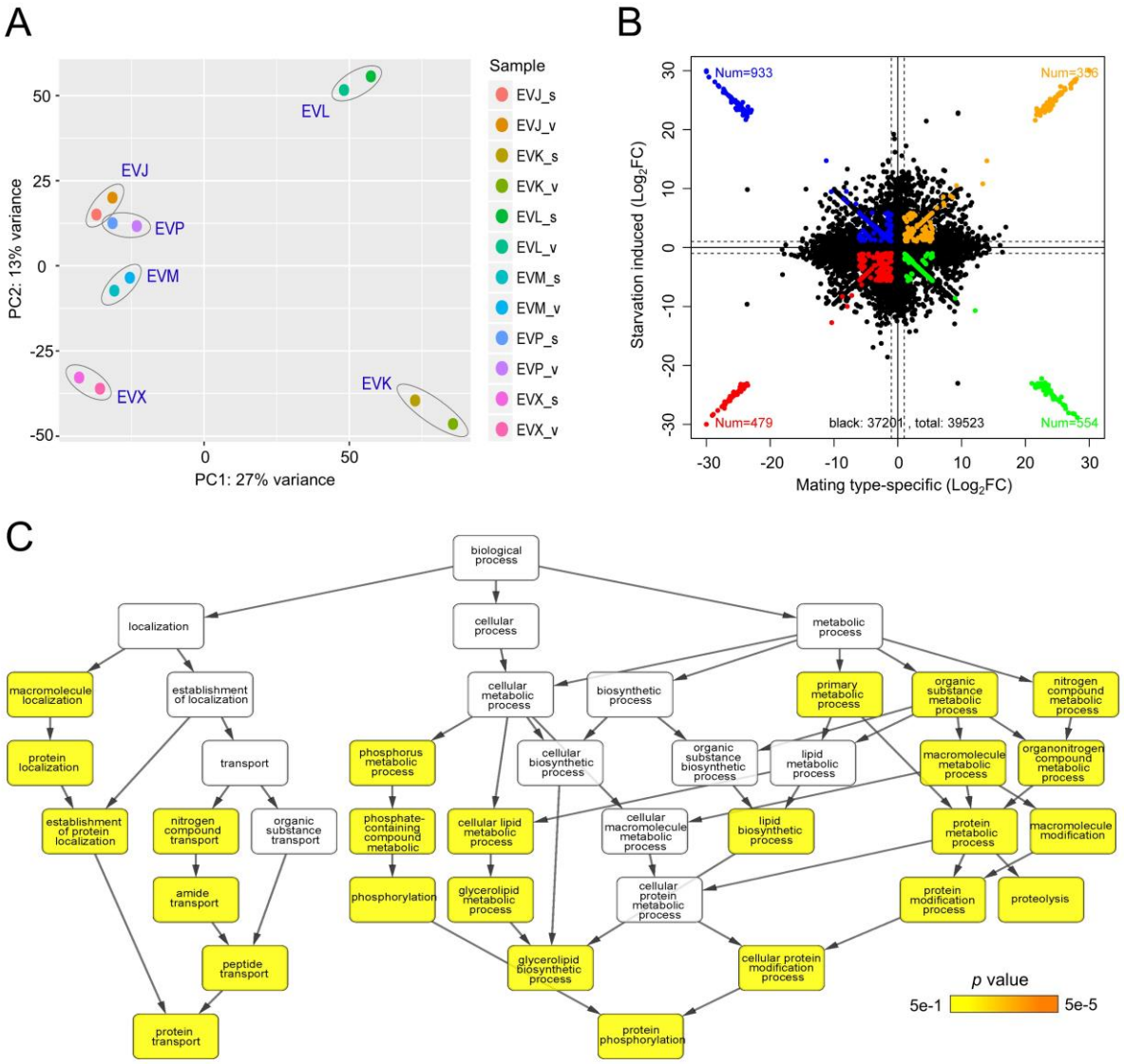

Figure 4. Gene function analysis of mating type-specific transcripts of *E. vannus*. (A) PCA analysis on transcript enrichment of different mating types. (B) Cross plot of differential expression of mating type-specific and starvation-regulated transcripts. (C) GO enrichment analysis of mating type-specific and starvation induced transcripts.

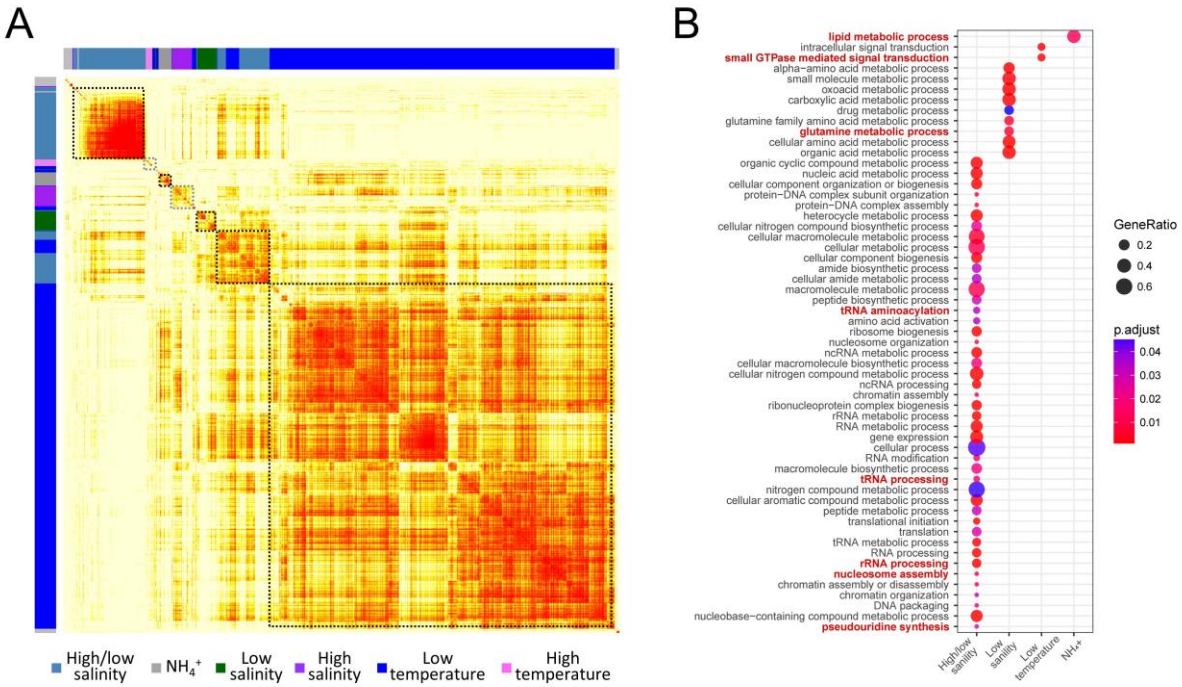

Figure 5. Differential gene expression analysis under temperature, salinity and free ammonia stresses. (A) Heatmap of weighted gene co-expression network, in accordance with different stress-response gene groups. (B) GO term enrichment analysis on different stress-response gene groups.

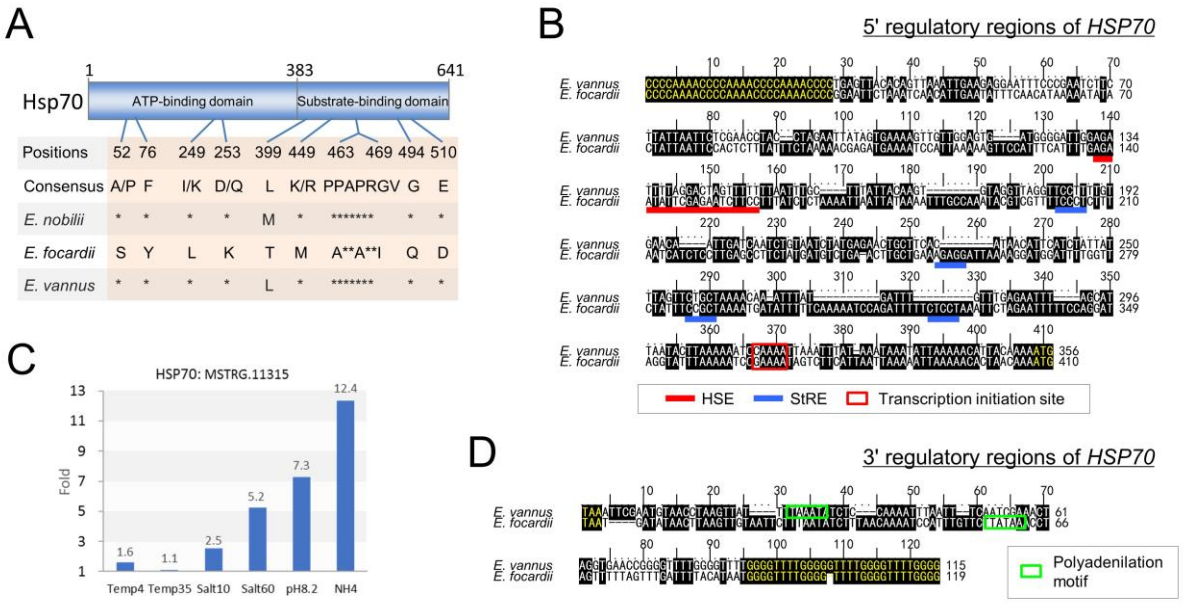

Figure 6. HSP70 gene expression analysis under temperature, salinity and free ammonia stresses. (A) Amino acid substitutions that occur in *E. focardii* at the level of its HSP70 ATP- and substrate-binding domains and are unique with respect to *E. nobilii* and other organisms. Asterisks denote identities. Numbers indicate essential amino acid positions of Hsp70. (B) Up-regulation folds in cells under different environmental stresses with respect to the control (25^{o}C, 35 psu and pH 7.8). (C) Nucleotide sequence alignment of the 5' regulatory regions of the *E. vannus* (gene "MSTRG.11315" on contig "Contig21532") and *E. focardii* HSP70 genes. The identities are shaded; the telomeric C4A4 repeats and transcription initiation ATG codons are in yellow; putative sites for the transcription initiation are boxed; sequence motifs bearing agreement with HSE and StRE elements are indicated by red and blue bars, respectively. (D) Nucleotide sequence alignment of the 3' regulatory regions of the *E. vannus* and *E. focardii* HSP70 genes. The identities are shaded; the telomeric G4T4 repeats and stop TAA codons are in yellow; putative polyadenylation motifs are boxed.

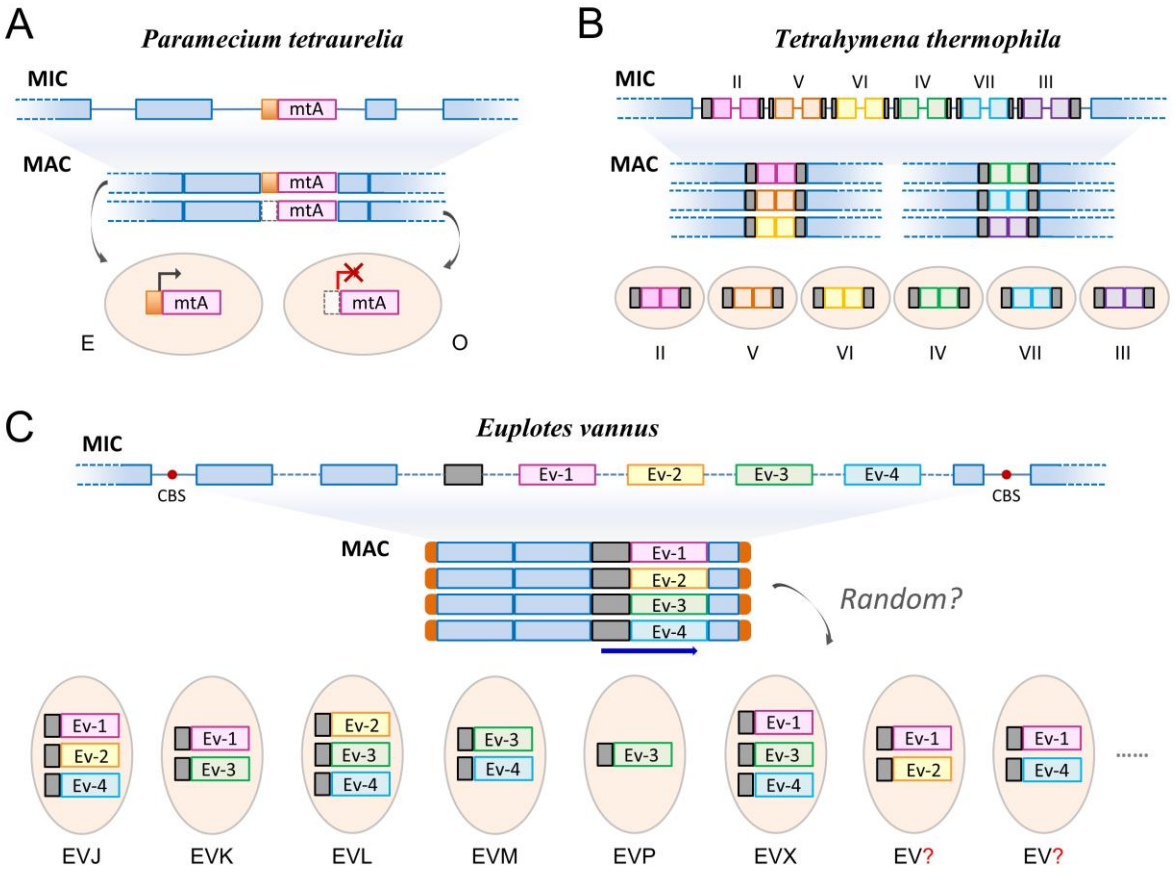

Figure 7. Current models (simplified) for mating type determination in *Paramecium tetraurelia*, *Tetrahymena thermophila* and *Euplotes vannus*. (A) One of the two *P. tetraurelia* mating types, mating type E depends on expression of the mtA gene during sexual reactivity. The other mating type O is determined during macronuclear development by excision of the mtA promoter (box in orange) as an internal eliminated sequence (IES), preventing expression of the gene. Adapted from Extended Data Figure 10 of Reference [41]. (B) Mating type gene pairs in *Tetrahymena thermophila* macronuclear are assembled by joining mating type-specific macronucleus destined sequence (MDS) from micronuclear to reproduce six mating types. Segments filled with grey represent conserved transmembrane regions. Adapted from Figure 3 of Reference [42]. (C) *E. vannus* shows a mating type-specific feature on the combination of different pheromone genes in MAC. Red dots denote chromosome breakage site (CBS). Segments filled with solid orange, light colors and grey denote telomeres, MDSs and conserved transmembrane regions, respectively. Dashed lines denote putative IESs.